Chemical Physics Letters 614 (2014) 220–225

Contents lists available at ScienceDirect

Chemical Physics Letters

journal homepage: www.elsevier.com/locate/cplett

Sensitivity improvement during heteronuclear spin decoupling in solid-state nuclear magnetic resonance experiments at high spinning frequencies and moderate radio-frequency amplitudes

Rudra N. Purusottam[a,b,c], Geoffrey Bodenhausen[a,b,c], Piotr Tekely[a,b,c,*]

[a] École Normale Supérieure – PSL Research University, Département de Chimie, 24, rue Lhomond, F-75005 Paris, France
[b] Sorbonne Universités, UPMC University Paris 06, LBM, 4 place Jussieu, F-75005 Paris, France
[c] CNRS, UMR 7203 LBM, F-75005 Paris, France

ARTICLE INFO

Article history:
Received 30 July 2014
In final form 15 September 2014
Available online 30 September 2014

ABSTRACT

Searching for optimal conditions during one- and multi-dimensional solid-state NMR experiments in high static fields may require spinning the sample at frequencies above 40 kHz. This implies challenging requirements for heteronuclear spin decoupling. We have compared the performance of the latest heteronuclear decoupling schemes at high magic-angle spinning frequencies. The results demonstrate that at commonly used *rf* amplitudes between 80 and 120 kHz, PISSARRO decoupling provides substantial sensitivity improvement. The performance of low-amplitude decoupling at different spinning speeds is also compared and its dependence on the inherent inhomogeneity of the *rf* field is probed by numerical simulations.

1. Introduction

Efficient heteronuclear decoupling is vital for obtaining high-resolution solid-state NMR spectra of low-gamma nuclei such as carbon-13. In polycrystalline and amorphous organic solids studied at magic-angle-spinning (MAS) frequencies above 5 kHz, flip-flop spin exchange between protons slows down and the efficiency of continuous-wave (CW) decoupling is not sufficient [1]. This disadvantage can be overcome by substituting CW irradiation by phase-alternated irradiation [1]. This was followed by the popular two-pulse phase-modulated (TPPM) technique [2] and its numerous variants [3–8] that have been successfully used for common spinning frequency ranges between 10 and 30 kHz. At high static fields, higher spinning frequencies may be preferred to attenuate residual spinning sidebands and unwanted rotational resonance effects that occur when an integer multiple of the spinning frequency ν_{rot} is roughly matched with the difference $\Delta\nu_{iso}$ between two isotropic chemical shifts ($n\nu_{rot} = \Delta\nu_{iso}$) [9]. This may lead to harmful line broadening or to undesirable magnetization exchange between specific sites. High spinning frequencies may also be useful at high static fields to create optimal conditions for broadband magnetization exchange in two-dimensional homonuclear correlation experiments [10]. Other indirect benefits of high spinning frequencies are related to the use of small-diameter rotors that allow one to run experiments with less than 1 mg powder sample. However, spinning frequencies around and above 30 kHz may also lead to a dramatic breakdown of the decoupling efficiency over a large range of *rf* amplitudes due to the phenomenon of rotary resonance recoupling (R^3) ($\nu_1 = n\nu_{rot}$) [11]. To overcome this complication, a phase-inverted supercycled sequence for attenuation of rotary resonance (PISSARRO) was developed and shown to be effective in quenching rotary resonance recoupling in the vicinity of $n = 2$ [12]. The method turned out also to achieve a very good decoupling efficiency at high *rf* amplitudes, far from any R^3 condition, as well as in the low-amplitude decoupling regime when $\nu_{rot} = 60$ kHz [13]. This is partially related to its capacity to make use of the modulation sidebands, which arise from the interference between the decoupling irradiation and the modulation of dipolar couplings by MAS [12]. A thorough analysis of the mechanism of quenching of rotary resonance recoupling effects by the PISSARRO scheme has revealed the crucial role of its mirror symmetry segments combined with phase-shifted irradiation [14]. The immunity of PISSARRO decoupling against the offsets of remote protons, their chemical shift anisotropies and second-order cross-terms between dipolar coupling and chemical-shift anisotropy has also been demonstrated [14,15]. Since the introduction of PISSARRO decoupling, a new class of pulse sequences, so-called refocused continuous-wave (rCW),

* Corresponding author at: École Normale Supérieure – PSL Research University, Département de Chimie, 24, rue Lhomond, F-75005 Paris, France.
E-mail address: Piotr.Tekely@ens.fr (P. Tekely).

http://dx.doi.org/10.1016/j.cplett.2014.09.044

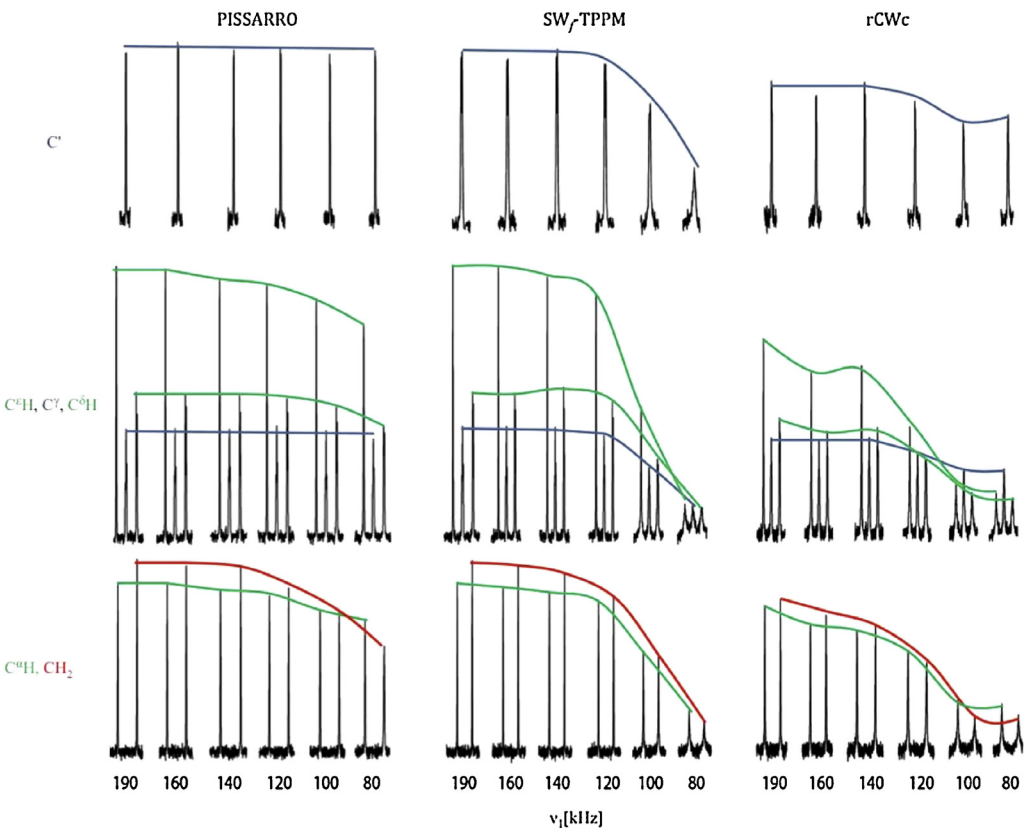

Figure 1. Comparison of the efficiency of heteronuclear decoupling for different carbons in L-histidine with PISSARRO (left), SW$_f$ -TPPM (middle) and rCWc (right) at B_0 = 9.4 T (400 MHz for protons) and ν_{rot} = 40 kHz as a function of the decoupling *rf* amplitude 190 > ν_1 > 80 kHz with the ^{1}H carrier frequency placed on-resonance for C$^{\alpha}$H. All spectra were recorded with 3.0 ms CP contact time, 8 scans and a 5 s recovery delay between experiments.

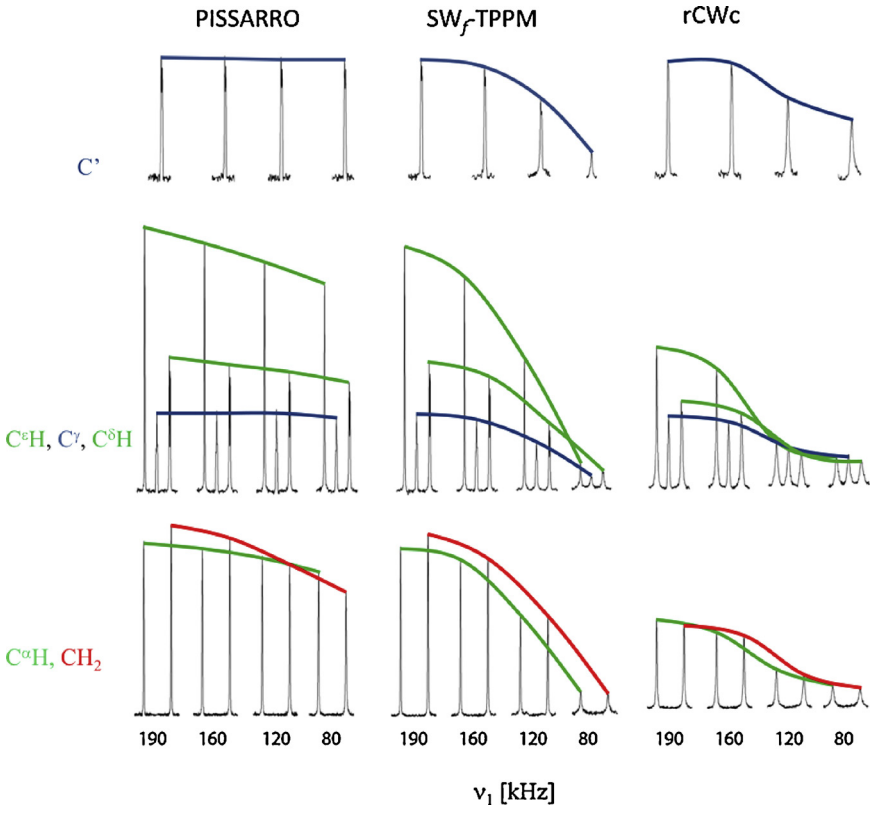

Figure 2. Same as in Figure 1 except that ν_{rot} = 60 kHz.

has been introduced [16]. Although rCW pulse sequences were so far only used for spinning frequencies up to 20 kHz, it has been suggested that they would also be efficient at high spinning speeds [17]. Independently, an amplitude-modulated XiX irradiation was proposed for the low-amplitude decoupling regime and tested at spinning frequencies of 60 and 90 kHz [18].

In this work, we show that at high spinning speeds, PISSARRO irradiation has a unique capacity to secure efficient decoupling at commonly used *rf* amplitudes between 80 and 120 kHz and provides significant sensitivity improvements. We also compare the efficiency of low-amplitude decoupling for lower spinning frequencies and point out the dependence of decoupling on the *rf* field inhomogeneity of the solenoid coil. For the sake of comparison, we also refer to the decoupling performance of SW_f-TPPM [6], which according to recent reports [19], offers improved efficiency over a larger range of *rf* amplitudes and spinning frequencies compared to its precursors.

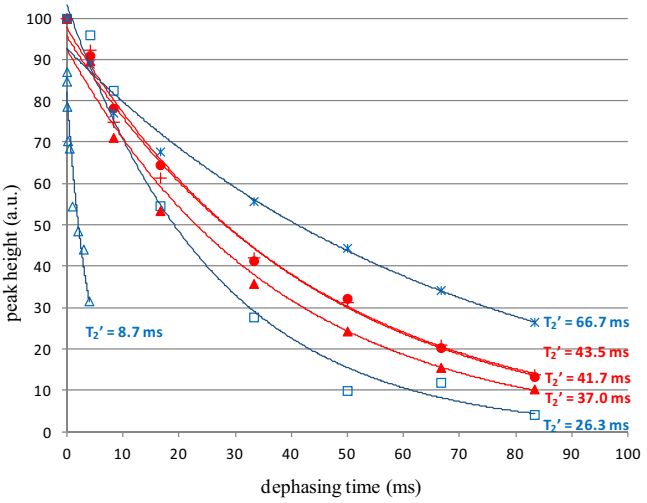

Figure 3. Echo decay curves for the $C^{\varepsilon}H$ carbon of L-histidine obtained using a single rotor-synchronized refocusing pulse at $B_0 = 9.4$ T and $\nu_{rot} = 60$ kHz. The SW_f-TPPM pulse sequence was used with *rf* decoupling amplitude of 160 (fx2), 120 (fx3) and 80 kHz (fx4). The T_2' relaxation times are respectively 66.7, 26.3 and 8.7 ms. The decays for PISSARRO at the same *rf* amplitudes are represented by red symbols (fx5, fx6 and fx7) and the corresponding T_2' values are 43.5, 41.7 and 37.0 ms. (For interpretation of the references to color in this figure legend, the reader is referred to the web version of this article.)

2. Experimental

Polycrystalline powders of uniformly ^{13}C, ^{15}N-labeled L-histidine hydrochloride monohydrate were used without further purification. All experiments were performed on a 400 MHz Bruker Avance II spectrometer and on a 850 MHz Bruker Avance III spectrometer, both equipped with double resonance CP/MAS probes using rotors with 1.3 mm diameter. For PISSARRO decoupling, only the pulse duration τ_p needs to be optimized in the vicinity of the recommended values, i.e. $\tau_p = 0.2\tau_{rot}$ for decoupling near the $n = 2$

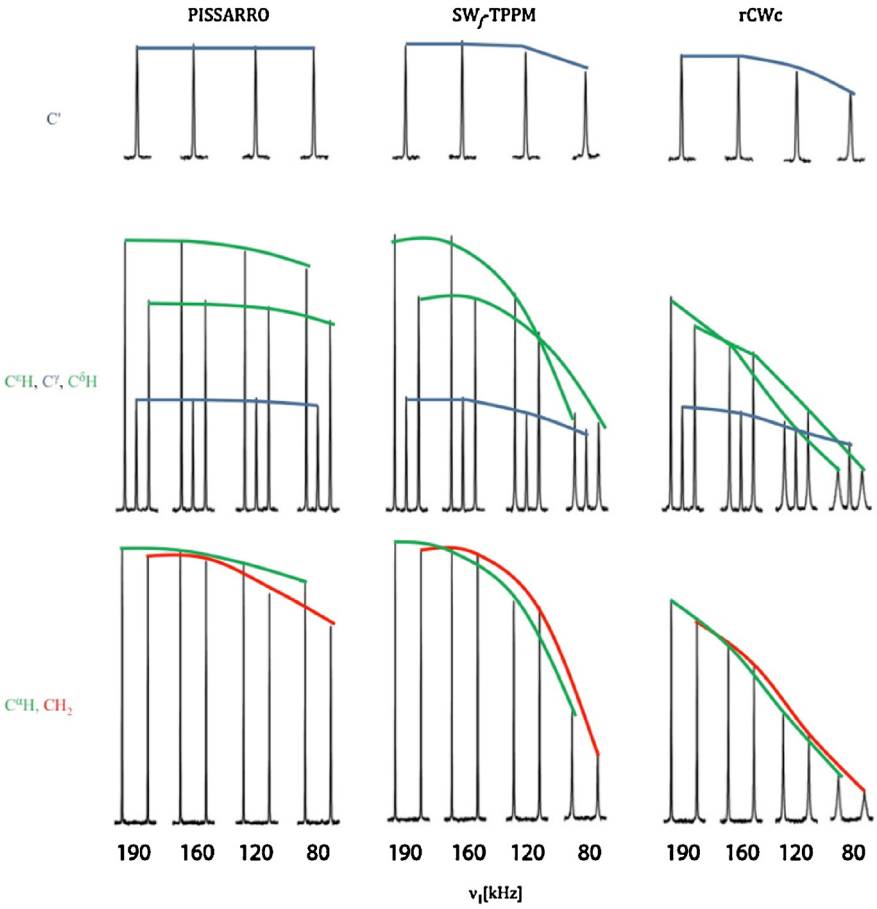

Figure 4. Comparison of the efficiency of heteronuclear decoupling for different carbons in L-histidine with PISSARRO (left), SW_f-TPPM (middle) and rCWc (right) at $B_0 = 19.9$ T (850 MHz for protons) and $\nu_{rot} = 60$ kHz as a function of the decoupling *rf* amplitude. All spectra were recorded after a pre-saturation of ^1H during 15.0 ms, 5 s relaxation delay, 1.3 ms CP contact time, 8 scans and 5 s delays between experiments.

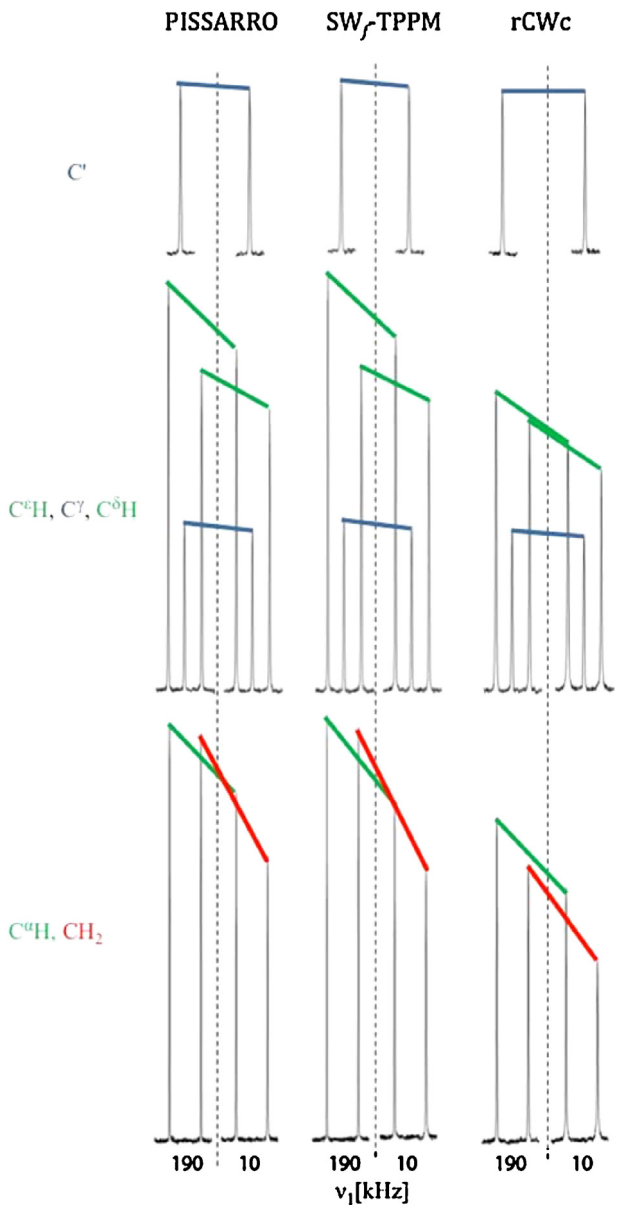

Figure 5. Comparison of the efficiency of heteronuclear decoupling for different carbons in L-histidine with PISSARRO (left), SW$_f$-TPPM (middle) and rCWc (right) at $B_0 = 19.9$ T and $\nu_{rot} = 60$ kHz in the high- and low-amplitude decoupling regime. Other parameters as in Figure 4.

rotary resonance condition, and $\tau_p = 0.9$ or $1.1\tau_{rot}$ for high *rf* amplitudes $\nu_1{}^H \gg 2\nu_{rot}$ [12]. For low-amplitude decoupling, the pulse lengths were optimized so that the nutation angles $\beta = 2\pi\nu_1\tau$ were in the vicinity of 6π [13]. For routine purposes, the pulse duration τ_p need not be optimized and may be safely fixed to the above-mentioned durations, depending on the spinning frequency and *rf* amplitude. This gives a major advantage of PISSARRO over current decoupling schemes. For SW$_f$-TPPM decoupling [6], optimum nutation angles were found in the range $120^\circ < \beta < 170^\circ$. The phase angle ϕ was optimized between 5° and 20° in steps of 2°. The number of pulse pairs was fixed to 11 and a linear sweep profile was applied. For rCW decoupling, we chose the rCWc version [16] for best performance under our experimental conditions and lower demands on *rf* field strengths. For the refocusing π pulses, an *rf* field amplitude of 220 kHz was used. The optimum continuous wave pulse length, i.e. the delay τ between the refocusing pulses, was around 50 μs ($\tau = n\tau_{rot}$, $n \cong 3$). For low-amplitude experiments recorded with the basic AM-XiX scheme [18], the XiX component was optimized empirically for various MAS frequencies ($\nu_1{}^H = 11.9$, 10.1, 8.6 kHz for $\nu_{rot} = 60$, 50 and 40 kHz MAS, respectively). The *rf* amplitude of the continuous wave component, as defined in [18], ranged between 2 and 3 kHz. The pulse length was optimized around $\tau_p \cong 5/2\tau_r$. Numerical simulations were carried out with SPINEVOLUTION [20], considering the 5-spin system $C^{\alpha}H^{\alpha}H^{\beta 1}H^{\beta 2}H^{N}$ of L-histidine hydrochloride monohydrate with internuclear distances derived from the crystallographic structure. In each case the pulse durations were optimized numerically in the vicinity of the recommended values.

3. Results and discussion

The performance of PISSARRO, SW$_f$-TPPM and rCWc at $\nu_{rot} = 40$ and 60 kHz in a medium static magnetic field ($B_0 = 9.4$ T) is compared in Figures 1 and 2 for all carbon-13 resonances of L-histidine.

A wide range of *rf* decoupling amplitudes $190 > \nu_1{}^H > 80$ kHz was tested. For 40 kHz MAS and high *rf* amplitudes between 190 and 120 kHz, PISSARRO and SW$_f$-TPPM offer similar performance, while lower peak heights are observed for rCWc. In contrast to PISSARRO, the other two methods show a significant drop of performance for $\nu_1{}^H < 120$ kHz. This drop is greatly amplified at $\nu_{rot} = 60$ kHz due to the destructive interference near the $n = 1$ and 2 rotary resonance conditions.

Although somewhat better decoupling for $\nu_1{}^H < 120$ kHz can be achieved with high-phase TPPM [21] than with SW$_f$-TPPM at $\nu_{rot} = 60$ kHz, the peak heights are only about 60–80% of those obtained with PISSARRO [15].

In ^{13}C spectra of organic solids recorded at high spinning frequencies and very high *rf* decoupling amplitudes, the observed line-widths are often not only determined by the performance of decoupling, but may be governed by the inhomogeneous distribution of isotropic chemical shifts and, to a lesser extent, by magnetic susceptibility, dynamic effects and minor instrumental misadjustments. By combining heteronuclear decoupling with spin echoes, one can determine the residual homogeneous line-width (also known as 'refocused line-width' characterized by the time constant T_2') that is relevant for many multipulse and multidimensional experiments [22,23]. To check to what extent T_2' is affected by the *rf* amplitude, we measured the echo decays of $^{13}C^{\varepsilon}H$, which is not involved in homonuclear J_{CC} couplings and has a total line-width $\delta H^*{}_{1/2} = 52.6$ Hz at $\nu_1{}^H = 160$ kHz. The longest ^{13}C T_2' is observed with SW$_f$-TPPM at $\nu_1{}^H = 160$ kHz. However, this does not translate into the highest peak of the $^{13}C^{\varepsilon}H$ resonance which is merely 86% of the peak height obtained with PISSARRO at the same decoupling amplitude. This corroborates earlier observations that the peak-heights and the line-widths are not simply inversely proportional to each other [14,22]. As shown in Figure 3, a significant drop of T_2' is observed with SW$_f$-TPPM when decreasing the *rf* amplitude. For $\nu_1{}^H = 160$, 120 and 80 kHz, we measured $T_2' = 66.7$, 26.3 and 8.7 ms, respectively. This translates into homogeneous line-widths at half-height $\delta H'_{1/2} = 4.8$, 12.1 and 36.6 Hz. The corresponding total line-widths with SW$_f$-TPPM were 53.5, 55.7 and 318.6 Hz. In contrast, the lifetimes measured with PISSARRO are largely independent of $\nu_1{}^H$ ($T_{2'} = 43.5$, 41.7 and 37.0 ms for $\nu_1{}^H = 160$, 120 and 80 kHz, respectively). These lifetimes provide satisfactory sensitivity without resorting to high *rf* amplitude. The corresponding homogeneous line-widths are 7.3, 7.6 and 8.6 Hz while the total line-widths are 52.6, 54.1 and 56.1 Hz.

Figure 4 shows the decoupling efficiency of PISSARRO, SW$_f$-TPPM and rCWc in high static magnetic field ($B_0 = 19.9$ T, or 850 MHz for protons) and $\nu_{rot} = 60$ kHz. Similar changes in decoupling performance as a function of $\nu_1{}^H$ as observed at low field (Figure 2) occur, except that the efficiency of SW$_f$-TPPM is

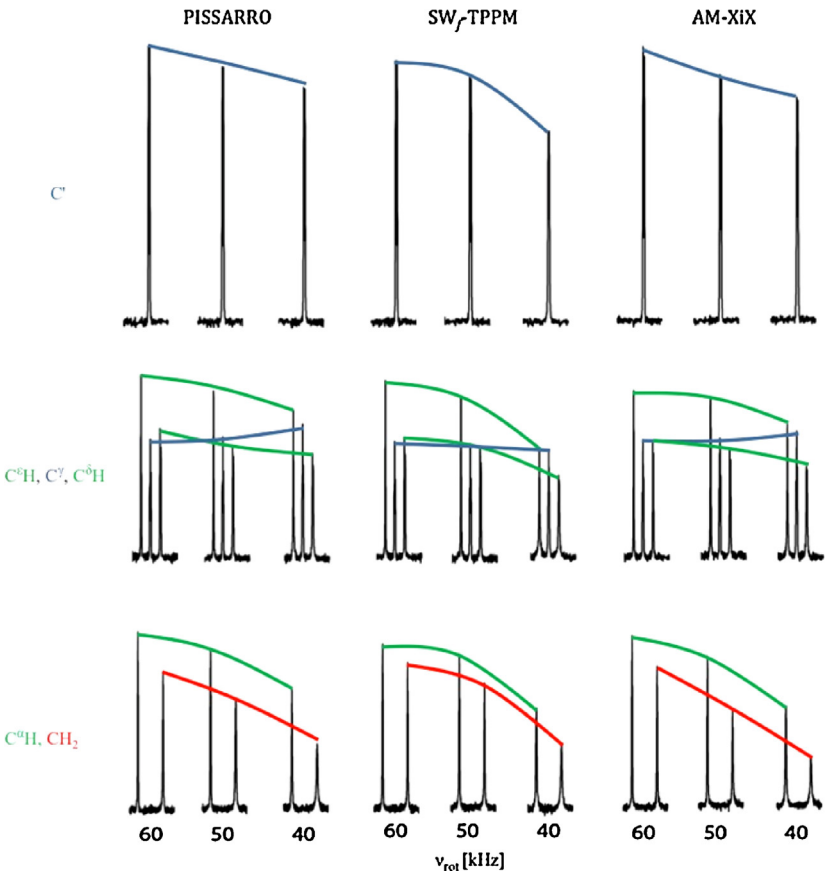

Figure 6. Comparison of the efficiency of low-amplitude heteronuclear decoupling for different carbons in L-histidine with PISSARRO (left), SW$_f$-TPPM (middle) and AM-XiX (right) at $B_0 = 9.4$ T and three spinning frequencies ν_{rot}. The optimized decoupling *rf* amplitudes ranged between 10 and 11 kHz to get the best efficiency in each case. All spectra were recorded with a single pulse experiment preceded by pre-saturation of ^{13}C during 15.0 ms and 5 s relaxation delay, 8 scans and 3 s delay between experiments. The observed increase of the intensity of a quaternary aromatic C$^{\gamma}$ carbon at the lowest spinning frequency results from its faster longitudinal relaxation.

somewhat improved near the $n = 2$ rotary resonance condition. The data corroborate a substantial sensitivity improvement with PISSARRO decoupling for commonly used *rf* amplitudes $80 < \nu_1{}^{H} < 120$ kHz over a wide range of static fields. This will help in high MAS experiments specifically designed to enhance the sensitivity, e.g., by promoting uniform Overhauser enhancements in ^{13}C NMR spectra of microcrystalline proteins [24].

Heteronuclear spin decoupling can also be efficient in a low *rf* amplitude regime with $\nu_1{}^{H} < 30$ kHz provided that $\nu_{rot} > 40$ kHz [7,13,18,25–27]. This allows a substantial reduction of the *rf* power dissipation, which may be vital for heat-sensitive samples. It has been demonstrated earlier that at $\nu_{rot} = 60$ kHz in a very high magnetic field $B_0 = 21$ T (900 MHz for protons), PISSARRO decoupling with $\nu_1{}^{H} = 15$ kHz has nearly the same efficiency as with $\nu_1{}^{H} = 150$ kHz for both CH_3 and CH resonances in alanine, while the peak height of CH_2 in glycine was 20% lower [13]. The comparison of peak heights shown in Figure 5 for L-histidine recorded at $B_0 = 19.9$ T and $\nu_{rot} = 60$ kHz in the high- and low-amplitude decoupling regimes reveals similar losses for various decoupling schemes.

For the sake of completeness, Figure 6 shows the peak heights of L-histidine recorded with PISSARRO, SW$_f$–TPPM and AM-XiX in the low amplitude regime ($10 < \nu_1{}^{H} < 11$ kHz) at $B_0 = 9.4$ T and at three spinning frequencies. The performance is nearly the same for all three pulse sequences, though slightly better for PISSARRO at $\nu_{rot} = 40$ kHz. More importantly, the observed loss of peak heights at lower spinning frequencies compels one to resort to *rf* amplitudes in the range of $80 < \nu_1{}^{H} < 100$ kHz where PISSARRO offers the best efficiency among current decoupling schemes.

All decoupling sequences use pulse durations that must be optimized for a given *rf* power. However, there is an unavoidable distribution of *rf* field amplitudes, mostly along the axis of the solenoid coil. To assess the consequences of this distribution on the performance of heteronuclear decoupling, the $^{13}C^{\alpha}H$ resonance

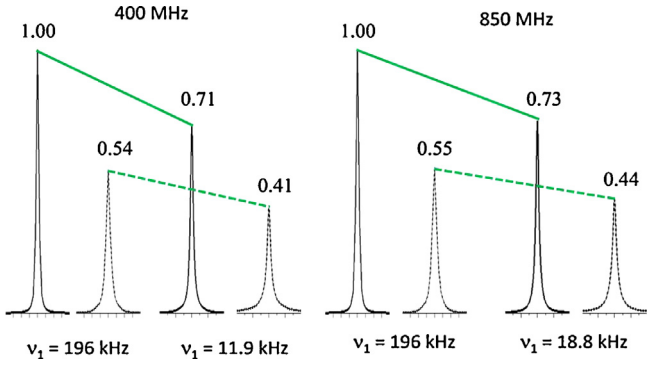

Figure 7. Numerically calculated $^{13}C^{\alpha}H$ lines, considering a spin cluster $C^{\alpha}H^{\alpha}H^{\beta 1}H^{\beta 2}H^{N1}$ in L-histidine with a high- and low-amplitude PISSARRO decoupling at $B_0 = 9.4$ T (left) and 19.9 T (right) and $\nu_{rot} = 60$ kHz. The lines were calculated assuming either a single *rf* amplitude (i.e., a perfectly homogeneous *rf* field, shown by solid lines) or a realistic distribution of *rf* fields calculated for a solenoid coil with an inner diameter of 1.5 mm and a length of 2.5 mm (dashed lines). The optimized high- and low-amplitude pulse durations were 18.48 μs ($1.109 * \tau_{rot}$) at both fields and 264.0 μs (corresponding to a nutation angle $\sim 3.14 \times 2\pi$) at 400 MHz and 218.16 μs (or nutation angle $\sim 4.1 \times 2\pi$) at 850 MHz. The resulting full-width at half-height (FWHH) ranged between 2.2 and 2.8 Hz for high- and low-amplitude decoupling, respectively.

line was calculated numerically, again considering a spin cluster $C^{\alpha}H^{\alpha}H^{\beta1}H^{\beta2}H^{N1}$ in L-histidine with high- and low-amplitude PISSARRO decoupling at 9.4 and 19.9 T and $\nu_{rot} = 60$ kHz (Figure 7).

The resonance lines were simulated assuming either a single *rf* amplitude (i.e., a perfectly homogeneous *rf* field) or a realistic distribution of *rf* field amplitudes, calculated using the Biot-Savart law for a solenoid coil with internal diameter of 1.5 mm and 2.5 mm length. The relative *rf* intensity ranges from 100% in the center of the coil to 56% at the edges. Interestingly, much better agreement with the experimental 16% drop of the $^{13}C^{\alpha}H$ peak height (Figure 5, left) is noted when assuming the relevant inhomogeneity of the *rf* field which leads to a 20% drop ($0.55 \rightarrow 0.44$), while with a homogeneous *rf* field it leads to a 27% drop ($1.0 \rightarrow 0.73$). More strikingly, when taking into account the inhomogeneity of the *rf* field, the drop of the peak heights is close to 45% for both high- and low-amplitude decoupling regimes and for both static fields. A similar decrease of intensity due to the *rf* field inhomogeneity is expected for other decoupling schemes. This reveals further potential for improving the sensitivity by designing new heteronuclear decoupling methods, especially in the low-amplitude regime, provided one can conceive a compensation for the *rf* field inhomogeneity. This little-explored aspect will be thoroughly examined elsewhere.

4. Conclusions

We have compared the performance of a few recent heteronuclear decoupling schemes at high magic-angle spinning frequencies where the choice of a particular scheme is not merely of academic interest but important for routine applications. The results show that at commonly used *rf* amplitudes $80 < \nu_1{}^{H} < 120$ kHz, the decoupling performance of PISSARRO compares favorably with other decoupling schemes and provides substantial sensitivity improvements. This is due to its unique capacity to quench efficiently rotary resonance recoupling near the $n = 2$ condition. Although a loss of intensity of about 15–25% is observed with current pulse sequences for low-amplitude decoupling at a spinning frequency $\nu_{rot} = 60$ kHz, compared to the high-amplitude regime, the losses are more pronounced at lower spinning frequencies. This compels one to resort to *rf* amplitudes $80 < \nu_1{}^{H} < 100$ kHz where PISSARRO decoupling reveals the best performance, compared with other currently used decoupling schemes, all of which need much higher *rf* amplitudes under such conditions to reach the same decoupling efficiency. We have also demonstrated by numerical simulations that for sample having an axial length equal to that of the solenoid coil, the inherent inhomogeneity of the *rf* field may lead to a decrease of the peak intensities by more than 40%, both in the high- and low-amplitude decoupling regimes. This suggests that further improvements could be achieved when dealing with fully packed rotors, by designed new schemes for heteronuclear decoupling with suitable compensation for the *rf* field inhomogeneity.

Acknowledgments

Financial support of the CNRS, the Ecole Normale Supérieure, the Université Pierre-et-Marie Curie (UPMC), the Ecole Doctorale ED388 (UPMC), the Equipex “Paris en Résonance”, the Fédération de Recherche (FR 3050) Très Grands Equipements de Résonance Magnétique Nucléaire à Très Hauts Champs (TGE RMN THC) of the CNRS and the European Research Foundation (ERC, project 339754 “Dilute para-water”) is gratefully acknowledged.

References

[1] P. Tekely, P. Palmas, D. Canet, J. Magn. Reson. A 107 (1994) 129.
[2] A.E. Bennett, C.M. Rienstra, M. Auger, K.V. Lakshli, R.G. Griffin, J. Chem. Phys. 103 (1995) 6951.
[3] Z. Gan, R.R. Ernst, Solid State NMR 8 (1997) 153.
[4] B.M. Fung, A.K. Khitrin, K. Ermolaev, J. Magn. Reson. 142 (2000) 97.
[5] K. Takegoshi, J. Mizokami, T. Terao, Chem. Phys. Lett. 341 (2001) 540.
[6] R.S. Thakur, N.D. Kurur, P.K. Madhu, Chem. Phys. Lett. 426 (2006) 459.
[7] M. Kotecha, N.P. Wickramasinghe, Y. Ishii, Magn. Reson. Chem. 45 (2007) S221.
[8] A. Equbal, S. Paul, V.S. Mithu, J.M. Vinther, N.C. Nielsen, P.K. Madhu, J. Magn. Reson. 244 (2014) 68.
[9] D.P. Raleigh, M.H. Levitt, R.G. Griffin, Chem. Phys. Lett. 146 (1988) 71.
[10] M. Weingarth, G. Bodenhausen, P. Tekely, Chem. Phys. Lett. 488 (2010) 10.
[11] T.G. Oas, R.G. Griffin, M.H. Levitt, J. Chem. Phys. 89 (1988) 692.
[12] M. Weingarth, P. Tekely, G. Bodenhausen, Chem. Phys. Lett. 466 (2008) 247.
[13] M. Weingarth, G. Bodenhausen, P. Tekely, J. Magn. Reson. 199 (2009) 238.
[14] M. Weingarth, G. Bodenhausen, P. Tekely, Chem. Phys. Lett. 502 (2011) 259.
[15] M. Weingarth, J. Trébosc, J.P. Amoureux, G. Bodenhausen, P. Tekely, Solid State NMR 40 (2011) 21.
[16] J.M. Vinther, A.B. Nielsen, M. Bjerring, E.R.H. van Eck, A.P.M. Kentgens, N. Khaneja, N.C. Nielsen, J. Chem. Phys. 137 (2012) 214202.
[17] J.M. Vinther, N. Khaneja, N.C. Nielsen, J. Magn. Reson. 226 (2013) 88.
[18] V. Agarval, T. Tuherm, A. Reinhold, J. Past, A. Samoson, M. Ernst, B.H. Meier, Chem. Phys. Lett. 583 (2013) 1.
[19] P.K. Madhu, Isr. J. Chem. 54 (2014) 25.
[20] M. Veshtort, R.G. Griffin, J. Magn. Reson. 178 (2006) 248.
[21] S. Paul, V.S. Mithu, J.M. Vinther, N.D. Kurur, P.K. Madhu, J. Magn. Reson. 203 (2009) 199.
[22] G. De Paëpe, A. Lesage, L. Emsley, J. Chem. Phys. 119 (2003) 4833.
[23] V.S. Mithu, S. Pratihar, S. Paul, P.K. Madhu, J. Magn. Reson. 220 (2012) 8.
[24] R.N. Purusottam, G. Bodenhausen, P. Tekely, J. Biomol. NMR 57 (2013) 11.
[25] M. Ernst, A. Samoson, B.H. Meier, Chem. Phys. Lett. 348 (2001) 293.
[26] M. Ernst, A. Samoson, B.H. Meier, J. Magn. Reson. 163 (2003) 332.
[27] V.S. Mithu, S. Paul, N.D. Kurur, P.K. Madhu, J. Magn. Reson. 209 (2011) 359.